
Multiscale Graph Comparison via the Embedded Laplacian Distance

Edric Tam¹ David Dunson¹

Abstract

We introduce a simple and fast method for comparing graphs of different sizes. Existing approaches are often either limited to comparing graphs with the same number of vertices or are computationally unscalable. We propose the Embedded Laplacian Distance (ELD) for comparing graphs of potentially vastly different sizes. Our approach first projects the graphs onto a common, low-dimensional Laplacian embedding space that respects graphical structure. This reduces the problem to that of comparing point clouds in a Euclidean space. A distance can then be computed efficiently via a natural sliced Wasserstein approach. We show that the ELD is a pseudo-metric and is invariant under graph isomorphism. We provide intuitive interpretations of the ELD using tools from spectral graph theory. We test the efficacy of the ELD approach extensively on both simulated and real data. Results obtained are excellent.

1. Introduction

Graphs and networks are ubiquitous objects in statistics, machine learning and related fields. A routine task in network analysis is graph comparison, which involves quantifying structural similarities between graphs. Graph comparison is a well-studied problem with an abundant literature. It has been used widely in the biomedical, social and engineering sciences, with application domains ranging from social network analysis to neural connectomics.

One of the main challenges in graph comparison is to develop simple, fast and theoretically sound methods for comparing graphs that are on different scales, i.e. graphs with different numbers of vertices. This is an important and natural task that arises in many application domains. For example, sociologists are often interested in comparing the structures of social communities with vastly different sizes

(Grindrod & Lee, 2016), while biologists might be interested in comparing protein-protein interaction networks between different species (Jeong et al., 2016). These applications naturally require comparison of graphs with different numbers of vertices. Beyond the scientific applications above, graph comparison can also serve as a foundational tool in many downstream machine learning and statistics tasks, such as graph classification (Richiardi et al., 2013), graph change-point detection (Sharpnack et al., 2013), graph hypothesis testing (Ginestet et al., 2017) and statistical modelling of network populations (Durante et al., 2017; Lunagómez et al., 2020). Better methods for multiscale graph comparison would extend the reach of many useful graph machine learning algorithms to the multiscale case.

Most existing approaches for graph comparison were designed for comparing graphs of the same size (in some cases requiring known vertex correspondence), often with no direct way to extend to the multiscale case. Existing methods that allow for multiscale comparison often suffer from a combinatorial growth in computational complexity, rendering them impractical in many scenarios. We highlight related approaches as well as their limitations in subsection 1.1.

Our contribution In this paper, we take a step towards addressing this gap. We introduce the embedded Laplacian distance (ELD), which provides a simple, fast and natural alternative to existing approaches. We provide theoretical characterizations for ELD, and illustrate its interpretation via spectral graph theory. We demonstrate the practical appeal via experiments. Our contributions are: 1) The embedded Laplacian distance is, to the best of our knowledge, the first method that combines a spectral/Laplacian embedding and a specialized sliced Wasserstein approach for comparing *collections* of graphs of different sizes. 2) We provide strong evidence, both theoretical and empirical, that supports the soundness and efficacy of this novel approach.

1.1. Related Work

There is an immense literature on graph comparison. Due to space limitations we only highlight those methods that are most relevant to our paper, and delegate the interested reader to the excellent reviews (Donnat & Holmes, 2018; Emmert-Streib et al., 2016; Wills & Meyer, 2020; Tantardini et al.,

¹Department of Statistical Science, Durham, NC 27705. Correspondence to: Edric Tam <edric.tam@duke.edu>.

2019; Soundarajan et al., 2014) for further information.

A predominant approach for graph comparison is via defining a pairwise graph distance. Distances that are based on the graph spectrum (Wilson & Zhu, 2008) or matrix representations (Wills & Meyer, 2020; Koutra et al., 2013) are generally confined to comparing graphs of the same sizes. Feature-based distances, for example those based on spectral or topological descriptors (Kaiser, 2011; Dehmer et al., 2010; Berlingerio et al., 2012), are less generalizable since they operate on a specified list of features and might ignore important graph information. The popular graph edit distances (Sanfeliu & Fu, 1983; Gao et al., 2010; Bunke, 1997), which are extensions of traditional string-based edit distances, have been shown to be NP-hard in general to compute (Zeng et al., 2009). Another approach for comparing graphs of different sizes is by considering graphs as metric spaces and then leveraging distances between isometry classes of metric spaces (Wills & Meyer, 2020), e.g. the Gromov-Hausdorff distance (Gromov, 2007; 1981; Edwards, 1975), the Wasserstein distance (Villani, 2009) etc. The Gromov-Hausdorff distance involves optimizing over isometric embeddings of metric spaces and is known to be NP-hard to compute (Chazal et al., 2009; Mémoli, 2007; Oles et al., 2019). A variety of methods using Wasserstein distances have been proposed for comparing graphs (Xu et al., 2019; Maretic et al., 2019; Vayer et al., 2018), although scalability remains a core issue. In the multiscale graph comparison context, one of the most recent methods is the Network Portrait Divergence (NPD) (Bagrow & Bollt, 2019), which uses information theoretic approaches to compare network portraits and is computationally fast. We compare the ELD against the NPD in our experiments.

Beyond graph distances, another predominant approach for graph comparison is graph kernels, which define an inner product between graphs, thus allowing use of kernel-based machine learning methods. Vishwanathan et al. (2010) provide a unified framework for many graph kernel methods, and Borgwardt et al. (2020); Kriege et al. (2020); Nikolentzos et al. (2019); Ghosh et al. (2018) provide recent surveys in this area. There are many variants with different emphasis, such as the random walk kernel, graphlet kernels, and shortest path kernels, to name a few. In the multiscale case, the direct product kernel (Gärtner et al., 2003; Ketkar et al., 2009) is often used. Given two graphs with m and n vertices respectively, this method constructs a direct product graph of size $O(mn)$, on which computation of the kernel could cost $O((mn)^3)$. This could be computationally burdensome in many practical applications.

There are several themes in the existing literature. Generally, methods that are based on global graph structure, such as the graph spectrum, do not directly extend to the multiscale scenario. Methods that are based on more lo-

cal, combinatorial structures, such as those that are based on matching subgraphs, graphlets, edit operations etc, usually run into computational bottlenecks, since at the core of these approaches lies the difficult problem of (sub)graph isomorphism.

1.2. Organization

The paper is organized as follows. In section 2, we set up the notation and preliminary notions from spectral graph theory and optimal transport that are needed for this paper. In section 3, we formally introduce the ELD. In section 4, we provide a theoretical characterization of the ELD. In section 5, we perform experiments on simulated and real graph data to illustrate the practical appeal of this approach. In section 6, we discuss the future directions and implications of this work.

2. Preliminaries

2.1. Notation and Setup

Let the triple $G = (V, E, w)$ denote a simple, undirected, weighted graph, where V is the set of vertices, $E \subset V \times V$ represents the edges of the graph, and $w : E \rightarrow \mathbb{R}_0^+$ is a weight function that assigns to each edge a non-negative real number. This framework subsumes the unweighted case, where we simply pick w to be a constant function on the edges. We use n to denote the number of vertices of G . Without loss of generality, we use the natural numbers to label the vertices, and denote by E_{ij} that edge that connects vertices i and j . We use $[n] := \{1, 2, \dots, n\}$ to denote the positive natural numbers up to n .

The graph’s adjacency matrix \mathbf{A} is the matrix with entries $\mathbf{A}_{ij} := w(E_{ij}) := w_{ij}$ if there is an edge between nodes i and j , and 0 otherwise. The degree matrix \mathbf{D} is the diagonal matrix with $\mathbf{D}_{ii} = \sum_{j=1}^n \mathbf{A}_{ij}$. The combinatorial Laplacian matrix \mathbf{L} is defined as $\mathbf{L} = \mathbf{D} - \mathbf{A}$. We use subscripts such as \mathbf{L}_G and \mathbf{A}_G to highlight dependency on the graph G . We use λ and \mathbf{v} to denote Laplacian eigenvalues and eigenvectors respectively. All matrices considered in the paper are symmetric, hence all corresponding eigenvalues are real. In particular, the combinatorial Laplacian matrix is positive-semidefinite, and its eigenvalues are presented in ascending order, so $0 \leq \lambda_i \leq \lambda_j$ for $i < j$.

2.2. Laplacian Embeddings

The core mathematical object in this paper is the combinatorial Laplacian matrix $\mathbf{L} = \mathbf{D} - \mathbf{A}$. It is used widely in spectral graph theory and manifold learning for tasks such as clustering and dimensionality reduction. One useful way to understand the graph Laplacian is to look at its eigendecomposition $\mathbf{L} = \sum_{i=1}^n \lambda_i \mathbf{v}_i \mathbf{v}_i^T$. As outlined in the seminal

paper (Belkin & Niyogi, 2003), this decomposition provides a natural Laplacian/spectral embedding of a graph’s vertices in Euclidean space: pick the first k eigenvectors (corresponding to the k smallest eigenvalues) of \mathbf{L} (where $k \in \mathbb{N}^+$ is a hyperparameter), and use the entries of these eigenvectors as Euclidean coordinates for embedding the vertices. In other words, the i^{th} entry of the k^{th} eigenvector $\mathbf{v}_k(i)$ provides the k^{th} coordinate of vertex i .

There are many ways to motivate and interpret the Laplacian embedding. The most relevant interpretation for our purposes is to see the Laplacian embedding as the solution to a natural optimization problem, due to Belkin & Niyogi (2003). Let $\mathbf{Y} := [\mathbf{y}_1 \cdots \mathbf{y}_k]$ be a $n \times k$ matrix, where \mathbf{Y}_{ij} represents the j^{th} Euclidean coordinate of the i^{th} vertex. If we want an embedding where vertices that are ”more connected” with each other are embedded closely, a natural objective function to minimize is $\sum_{(i,j) \in E} w_{ij} \|\mathbf{y}(i) - \mathbf{y}(j)\|^2 = \text{Tr}(\mathbf{Y}^T \mathbf{L} \mathbf{Y})$, which is simply a weighted least squares minimization problem. We then have the following result:

Theorem 2.1 (Optimal Linear Embedding (Belkin & Niyogi, 2003)). *Given a connected graph $G = (V, E, w)$, the solution $\mathbf{Y} = [\mathbf{y}_1 \cdots \mathbf{y}_k]$ of the following optimization problem*

$$\arg \min_{\mathbf{Y}; \mathbf{Y}^T \mathbf{Y} = \mathbf{I}} \text{Tr}(\mathbf{Y}^T \mathbf{L} \mathbf{Y})$$

corresponds to the first k Laplacian eigenvectors.

Here the constraint $\mathbf{Y}^T \mathbf{Y} = \mathbf{I}$ enforces orthonormality. The proof’s arguments are based on standard spectral graph theory and the Rayleigh-Ritz variational characterization of eigenvalues, and can be found in references such as (Belkin & Niyogi, 2003). Optionally, one can ignore the first eigenvector, which will always be constant.

The loss function above is set up in such a way that the Laplacian embedding respects graph connectivity, since vertices that are ”more connected” with each other are embedded more closely. To see this more concretely, consider graphs that exhibit community/cluster connectivity patterns. It is well known that the Laplacian embedding capture such cluster structures faithfully. The Laplacian embedding serves as the foundation of popular algorithms, such as spectral clustering (Ng et al., 2001; Von Luxburg, 2007; Shi & Malik, 2000). The intuition is that since ”more connected” vertices are embedded closer together, one can just run Euclidean clustering algorithms (e.g. K-means) in the embedding space to recover graph clusters. The fact that Laplacian embeddings capture cluster structures is rigorously justified by results in spectral graph theory known as higher-order Cheeger’s inequalities (Lee et al., 2014; Louis et al., 2012). Such results imply that if the vertices of a graph admit k sparse cuts, then the resulting k partitions can be captured by the first k Laplacian eigenvectors of the graph.

In summary, if we want to compare graphs based on their connectivity patterns (in particular whether the graphs exhibit similar clustering structures), it is natural to consider the Laplacian embedding as a starting point. The embedding dimension k will serve as a hyperparameter that controls the number of clusters we are taking into consideration.

In subsequent sections, we will adopt the notation $\mathbf{\Gamma}_k : G \rightarrow \mathbb{R}^{n \times k}$ to denote the embedding that maps a graph G to a set of n points in k -dimensional Euclidean space. Note that each eigenvector is determined only up to sign. To fix the orientations, we adopt the convention of picking the version of each eigenvector that has the larger lexicographic order.

2.3. Wasserstein and Sliced Wasserstein Distances

The Laplacian embedding introduced above turns graphs into point clouds in Euclidean space. A natural way to compare point clouds is via Wasserstein distances, which define metrics between probability measures. They are intimately connected to optimal transport (Villani, 2009), and have been used in graph settings increasingly often (Saad-Eldin et al., 2021; Kolouri et al., 2020).

One notable use of Wasserstein distances is to define a metric between sets of points in k -dimensional Euclidean space. This is done via defining an empirical probability measure for each set of points and computing the Wasserstein distance between them. Formally, given the sets of points $\mathcal{X} = \{\mathbf{x}_1, \mathbf{x}_2, \dots, \mathbf{x}_n | \mathbf{x}_i \in \mathbb{R}^k \forall i \in [n]\}$ and $\mathcal{Y} = \{\mathbf{y}_1, \mathbf{y}_2, \dots, \mathbf{y}_m | \mathbf{y}_j \in \mathbb{R}^k \forall j \in [m]\}$, define the empirical measures $\mu_{\mathcal{X}} = \frac{1}{n} \sum_{i=1}^n \delta_{\mathbf{x}_i}$ and $\nu_{\mathcal{Y}} = \frac{1}{m} \sum_{j=1}^m \delta_{\mathbf{y}_j}$. Overloading notation, we can then define the Wasserstein distance between the sets of points as:

$$W_p(\mathcal{X}, \mathcal{Y}) := W_p(\mu_{\mathcal{X}}, \nu_{\mathcal{Y}})$$

$$:= \inf_{J \in \mathcal{J}(\mu_{\mathcal{X}}, \nu_{\mathcal{Y}})} \left(\int_{\mathbb{R}^k \times \mathbb{R}^k} d(x, y)^p dJ(x, y) \right)^{1/p}$$

where $\mathcal{J}(\mu_{\mathcal{X}}, \nu_{\mathcal{Y}})$ denotes the set of all couplings of $\mu_{\mathcal{X}}$ and $\nu_{\mathcal{Y}}$, and $p \geq 1$ specifies the order of the moment used.

For cases where $k > 1$, computing the exact Wasserstein distance can involve time-consuming optimization that hampers computational performance. This computational problem largely disappears in the case of 1-dimensional distributions, where W_p admits equivalent analytic formulations that can be computed very efficiently.

This has motivated various methods to define distances between higher-dimensional distributions/point clouds with one dimensional marginals/”slices” in lieu of the full Wasserstein distance. The sliced Wasserstein distance is one such approach (Rabin et al., 2011; Bonneel et al., 2015; Kolouri et al., 2019; Nadjahi et al., 2021). Given two measures μ and ν , along with S sample directions $\{\phi_s\}_{s=1}^S$ usually drawn

uniformly from the unit sphere, it computes 1D Wasserstein distances between the measures' marginals along the sample directions and averages over them. In other words, $\mathcal{SW}_p(\mu, \nu) := \frac{1}{S} \sum_{s=1}^S \mathcal{W}_p(\text{proj}_{\phi_s}(\mu), \text{proj}_{\phi_s}(\nu))$, where $\text{proj}_{\phi_s}(\mu)$ denotes the 1D projection of the measure μ along ϕ_s .

While it allows for much faster computation while retaining certain desirable properties (Bonnotte, 2013), the sliced Wasserstein distance introduces an extra degree of noise to the problem which is undesirable in our setting. In the next section, we introduce a simple, fast and deterministic version of the sliced Wasserstein distance that is particularly suitable for our setting, which we combine with the Laplacian embedding to define the Embedded Laplacian Distance.

3. The Embedded Laplacian Distance (ELD)

We now formally introduce the ELD. Let \mathcal{G} denote the space of all simple, undirected, weighted graphs with finite numbers of vertices. Our goal is to construct a mapping $\rho : \mathcal{G} \times \mathcal{G} \rightarrow \mathbb{R}_0^+$ that quantifies the structural similarity/dissimilarity between two graphs. We will do so by first using the Laplacian embedding to transform the two graphs into two sets of points in a *common* k -dimensional Euclidean space. We will then compute a sliced Wasserstein distance that only slices along the k canonical Euclidean axes.

Definition 3.1 (Embedded Laplacian Distance). Consider two graphs $G_1 = (V_1, E_1, w_1) \in \mathcal{G}$ and $G_2 = (V_2, E_2, w_2) \in \mathcal{G}$, with sizes $n_1 := |V_1|$ and $n_2 := |V_2|$ and Laplacians L_{G_1} and L_{G_2} respectively. Without loss of generality we assume $n_1 \leq n_2$. Let $\mathcal{E} = \{\mathbf{e}_1, \dots, \mathbf{e}_k\}$ be the first k canonical Euclidean basis vectors. Define the embedded Laplacian distance as

$$\rho(G_1, G_2) := \frac{1}{k} \sum_{r=1}^k \mathcal{W}_p(\lambda_r^{G_1} \text{proj}_{\mathbf{e}_r}(\mu_{\Gamma_k(G_1)}), \lambda_r^{G_2} \text{proj}_{\mathbf{e}_r}(\nu_{\Gamma_k(G_2)}))$$

where Γ_k denotes the k -dimensional Laplacian embedding map. We use the notation ρ_k when we want to emphasize k .

Several remarks are in order. First, Laplacian embeddings have traditionally been used in the context of analyzing vertices/clusters in a single graph. One of our contributions is we realize that Laplacian embeddings could be used to project *collections* of graphs with different sizes onto a *common* Euclidean space. Second, since the point clouds live on a common Euclidean space, it is natural to compare them only along the canonical Euclidean axes \mathcal{E} , which are orthogonal and together span the space. This leads to the definition of $\mathcal{SW}_p^{\mathcal{E}}$, which enjoys several properties. 1. it

is deterministic 2. slicing along Euclidean basis vectors allows us to directly extract the entries of the Laplacian eigenvectors as coordinates. 3. it leads to the ELD being isomorphism invariant (see theorem 4.2 below).

Third, we weight each term inside the sliced Wasserstein distance by the corresponding Laplacian eigenvalues of the graphs, which puts the entries of the Laplacian eigenvectors under their natural scalings.

Here, k is a hyperparameter that determines the dimension of the embedding Euclidean space, as discussed in section 2.2. We require that $k \leq \min(n_1, n_2)$ in order for the embedding to be well-defined. In practice, we recommend picking k to be the largest possible under one's computational budget. For downstream applications in supervised learning, k can be chosen via cross-validation.

3.1. Computation of the ELD

We provide a procedure for implementing the ELD in Algorithm 1. In terms of computational complexity, the dominating step is the eigendecomposition, which is of order $O(n_2^3)$ under a naive theoretical analysis. In practice, most of the time $k \ll n$ and the eigendecomposition can be sped up via sparse or approximate numerical schemes, as discussed in section 6.

Algorithm 1 Embedded Laplacian Distance

- 1: **Input:** Two graphs $G_1 = (V_1, E_1, w_1)$ and $G_2 = (V_2, E_2, w_2)$ with $|V_1| = n_1$ and $|V_2| = n_2$
 - 2: **Output:** A non-negative real number $\rho(G_1, G_2)$ that quantifies the structural similarity between G_1 and G_2
 - 3: **Hyperparameters:** Positive integers $k \leq \min(n_1, n_2)$, and $p \geq 1$
 - 4: **Algorithm:**
 - 5: Compute the Laplacians L_{G_1} and L_{G_2}
 - 6: Compute the eigendecomposition of L_{G_1} and L_{G_2} to obtain the Laplacian eigenvalues/eigenvectors of each graph $\{\lambda_i^{G_1}, \mathbf{v}_i^{G_1}\}$ and $\{\lambda_j^{G_2}, \mathbf{v}_j^{G_2}\}$
 - 7: Take the first k eigenvectors $\{\mathbf{v}_i^{G_1}\}_{i=1}^k$ and $\{\mathbf{v}_j^{G_2}\}_{j=1}^k$ of each graph corresponding to the smallest k eigenvalues.
 - 8: Construct Euclidean points $\{\mathbf{x}_1^{G_1}, \dots, \mathbf{x}_{n_1}^{G_1}\} \subset \mathbb{R}^k$ and $\{\mathbf{y}_1^{G_2}, \dots, \mathbf{y}_{n_2}^{G_2}\} \subset \mathbb{R}^k$, where the r th coordinate of the i th vertex from G_1 will be $\mathbf{x}_i^{G_1}(r) := \mathbf{v}_r^{G_1}(i)$. Ditto for vertices in G_2 .
 - 9: Construct 1D empirical measures for each Euclidean dimension. In other words, for each $r \in [k]$, compute: $\mu_{\mathcal{X}}^r = \frac{1}{n_1} \sum_{i=1}^{n_1} \delta_{\lambda_r^{G_1} \mathbf{x}_i^{G_1}(r)}$ and $\nu_{\mathcal{Y}}^r = \frac{1}{n_2} \sum_{j=1}^{n_2} \delta_{\lambda_r^{G_2} \mathbf{y}_j^{G_2}(r)}$
 - 10: For each $r \in [k]$, compute the 1D Wasserstein distance $\mathcal{W}_p(\mu_{\mathcal{X}}^r, \nu_{\mathcal{Y}}^r)$
 - 11: Return the average $\rho = \frac{1}{k} \sum_{r=1}^k \mathcal{W}_p(\mu_{\mathcal{X}}^r, \nu_{\mathcal{Y}}^r)$
-

4. Theoretical Properties

We now demonstrate some mathematical properties of the ELD in this section. We first show that the ELD is a pseudometric.

Theorem 4.1 (Pseudometric Property). *The embedded Laplacian distance $\rho : \mathcal{G} \times \mathcal{G} \rightarrow \mathbb{R}^+$ is a pseudo-metric.*

Proof. See section A.1 in the appendix. \square

For our purposes of multiscale comparison, the pseudometric property is appropriate and it is in general not feasible to upgrade the ELD to a metric. Since the goal of the ELD is to capture graph structure, isomorphic graphs will have a distance of 0 between each other under the ELD, thus preventing the realization of the identity of indiscernibles property of metrics. Even if we only consider defining a distance between equivalent classes of isomorphic graphs, the fact that the graphs could be of different sizes renders the identity of indiscernibles property generally impossible since the smaller graph has less degrees of freedom than the larger graph.

We now show that the ELD is invariant to graph isomorphisms, i.e. permutations of the vertices that preserve edge structure. Given any permutation $\sigma : [n] \rightarrow [n]$, we can associate to it a permutation matrix \mathbf{P}_σ , and we use G_σ to denote the graph obtained by applying σ on the vertices of G .

Theorem 4.2 (Invariance to Graph Isomorphisms). *The embedded Laplacian distance $\rho : \mathcal{G} \times \mathcal{G} \rightarrow \mathbb{R}^+$ is invariant to permutations. I.e. given graphs G and H with n_1 and n_2 vertices respectively, given permutations σ on $[n_1]$ and ω on $[n_2]$, we have:*

$$\rho_k(G, H) = \rho_k(G_\sigma, H_\omega)$$

for any integer $k \leq \min(n_1, n_2)$.

Proof. See section A.2 in the appendix. \square

The invariance under isomorphism property ensures that the ELD is only capturing the desired graph connectivity structure, rather than non-structural characteristics of the graphs that depend on arbitrary vertex labels.

5. Experiments and Results

To gauge the efficacy of the ELD approach in practice, we implemented the ELD algorithm in Python 3.8 and tested it on both simulated and real datasets. We have included source code for replicating the experiments/figures in the supplementary materials. All experiments were conducted on a Unix machine with 8GB of RAM and an Intel i7 8-core processor. The software to reproduce all experiments

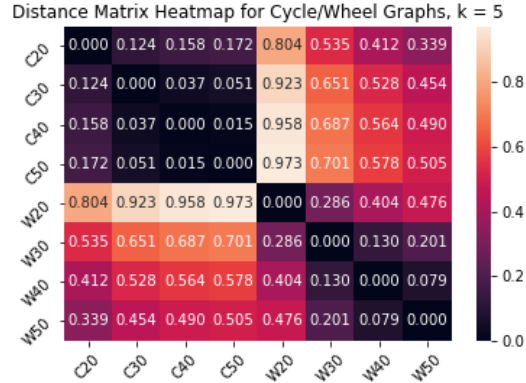


Figure 1. Heatmap of ELD Distance matrix between cycle graphs and wheel graphs

in this paper is available at <https://github.com/edriam/Embedded-Laplacian-Distance>. In all experiments below, we choose $p = 1$ for simplicity. Varying the p parameter of the Wasserstein distance does not impact the general conclusions of our experiments.

Simulated Data: Unweighted Graphs Since there is no groundtruth distance between graphs, the most natural way to evaluate the ELD is by simulating graphs from different families, showing that the ELD between graphs sharing structural similarities are small, whereas the ELD between graphs with differing structures is large.

In figures 1 and 2, we use the ELD to evaluate several families of graphs and generate distance matrices. We use W, C, R to denote wheel graphs, cycle graphs and rings of cliques, respectively. The numbers after W, C indicate the number of vertices in these graphs, whereas the numbers after R indicate the number of cliques and the clique size respectively.

In these figures we observe patterns in the distance matrices that fit our intuitive understanding of graph structures. Both subfigures show clear block structures that match with the types of graphs under consideration. The choices of k here is 5 for figure 1 and 9 for figure 2 (because the number of vertices of $R3, 3$ is 9, so that is the maximal allowable k). The block structures that we observe in the distance matrices are preserved when k is varied.

Simulated Data: Weighted Graphs In figure 3 and 4, we used the ELD to evaluate weighted graphs. We generated various random weighted graphs from Erdős-Rényi (ER) models with different connection probabilities and edge weights sampled from different exponential distributions. The goal of this simulation is to test whether the ELD

Distance Matrix Heatmap for Ring of Cliques Graphs, $k = 9$

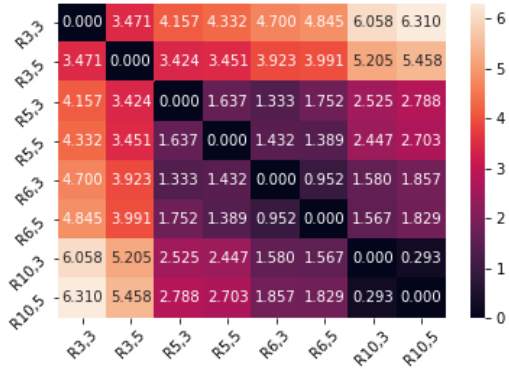


Figure 2. Heatmap of ELD Distance matrix between rings of cliques

is sensitive to edge-weight-induced connectivity differences between graphs from different scales. The number of vertices of the graph, the edge probability of the ER model and the scale parameter of the exponential distributions were varied and resulting graphs were compared. We used $k = 5$ in figure 2, but similar block structures are observed when we vary k .

In figure 3, we fixed the scale parameter of the exponential distribution at 20, and compared ER graphs with 20 and 100 nodes with edge probability 0.2 and 0.8. We included two samples from each of these 4 configurations, and the resulting distance matrix showed clear block structure which demonstrates ELD’s ability to distinguish between weighted ER graphs with different edge probabilities across different scales.

In figure 4, we fixed the edge probability parameter at 0.5, and compared ER graphs with 20 and 100 nodes with exponential scale parameter 2 and 30. We included two samples from each of these 4 configurations, and again the resulting block structures shows that the ELD can distinguish between ER graphs across scales with different weight distributions.

Comparison with other methods We explore the efficacy of the ELD in comparison to other existing distances between graphs of different scales. One of the most cited and influential approaches for this is the graph edit distance (GED) (Sanfeliu & Fu, 1983). Another competitor is the Network Portrait Divergence (NPD) (Bagrow & Bollt, 2019), which is one of the most recent contributions to this area. We discovered that the computational time for the GED (using an implementation from the popular NetworkX library (Hagberg et al., 2008)) exceeded our computational budget even for moderate-sized networks, e.g. graphs with several hundred vertices. In terms of computational speed in

Distance Matrix: ER graphs w/ Exp. Dist. Weights, $k = 5$

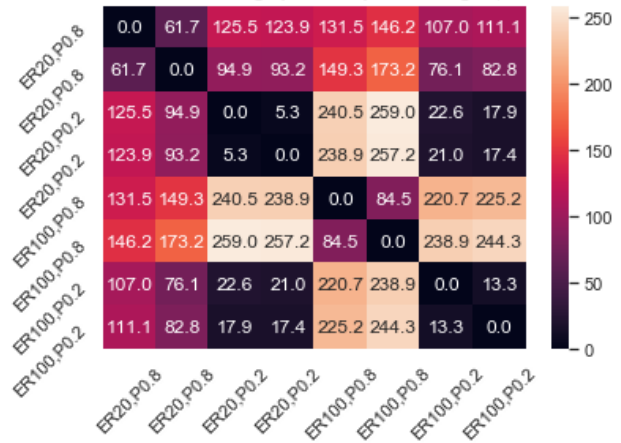


Figure 3. Heatmap of ELD Distance matrix between weighted ER graphs (varying edge probability)

Distance Matrix: ER graphs w/ Exp. Dist. Weights, $k = 5$

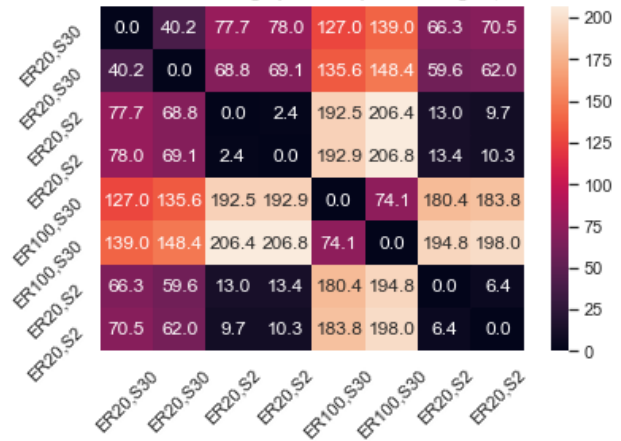


Figure 4. Heatmap of ELD Distance matrix between weighted ER graphs (varying scale parameter for weight distribution)

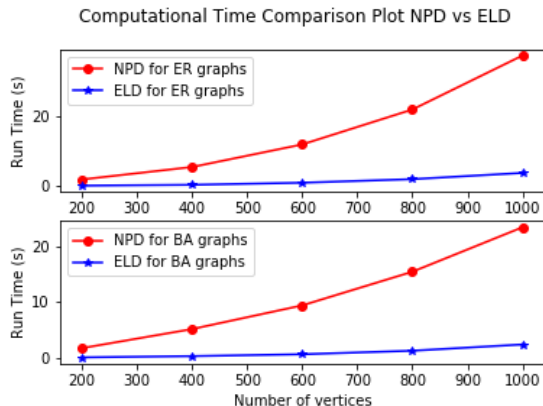


Figure 5. Computational time of NPD and ELD

practice, the ELD exceeds the GED by orders of magnitude. We therefore compared only the NPD and ELD.

We generated 10 samples from two random graph models: 1) Erdős-Rényi graphs with edge probability 0.03 and 2) Barabasi-Albert (BA) graphs with edge parameter 3. We computed the total running time for NPD and ELD on both these models with varying number of vertices, and results are shown in figure 5. To prevent the choice of k from affecting the results, in our implementation we computed the full eigendecomposition in ELD. We observe that the ELD significantly outperforms the NPD in terms of computational speed, often faster by a factor of ≥ 10 . As the sizes of the graphs grow, the computational advantage of ELD becomes more substantial. We find that for large graphs (≥ 10000) vertices, using the sparse implementation of ELD (provided in supplementary code) provides even more speedup.

In figure 6 we computed the NPD distance matrix on the same family of rings of cliques graphs in figure 2. While the ELD distance matrix in figure 2 demonstrated clear block structures, the NPD distance matrix in figure 6 did not. We discuss figure 6 further in our discussion. Taken together, these results show the practical appeal of the ELD in capturing meaningful similarities between graph structures as well as in computational speed.

Real Data For real network data, we used a temporal collaboration network dataset from Bagrow & Bollt (2019), as well as connectome data hosted at NeuroData (Vogelstein et al., 2018).

The connectome data we used consisted of graphs characterizing different regions of the brain from different organisms, including two graphs from mice (Bock et al., 2011), three from rats (Bota et al., 2012) and two from the nematode *P. pacificus* (Bumbarger et al., 2013). The connectome graphs are directed, and we take their undirected underlying graphs

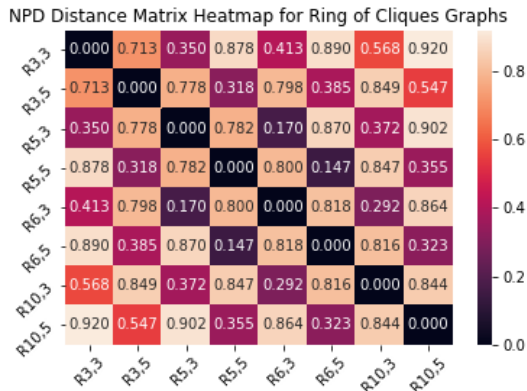


Figure 6. Heatmap of NPD Distance matrix between rings of cliques

for comparison in figure 7.

The collaboration network dataset contains 5 graphs, one from each year between 2013-2017, that documents the collaborations between developers on open-source IBM software hosted on Github. The nodes represents developers, and the edges between nodes indicate whether two developers have collaborated on at least one project. The graphs contain more nodes and edges over the years as more developers and collaborations occur. We compare these 5 graphs in figure 8.

In both figures, we observe that the ELD captures relevant graph structural information. There are clear block structures that distinguishes between the connectome graphs of different organisms in figure 7. In figure 8 there is a clear gradual pattern emerging in the collaboration network dataset, showing that graphs that are temporally closer are also structurally more similar, which matches the generation mechanism of the dataset.

6. Discussion and Future Directions

The motivation of the ELD is to offer a principled and practical way for comparing graphs that might have similar structures but different sizes, which often arises in applications. Note that comparing graphs of the same size is simply a special case of the ELD framework we presented, so all of our theoretical guarantees and computer programs carry over. The framework that we presented mainly deals with (weighted) simple, undirected graphs, but ELD could be potentially extended to many settings. We discuss two of these directions below.

Directed Graphs ELD could potentially be generalized to comparing directed graphs. One way is to apply the

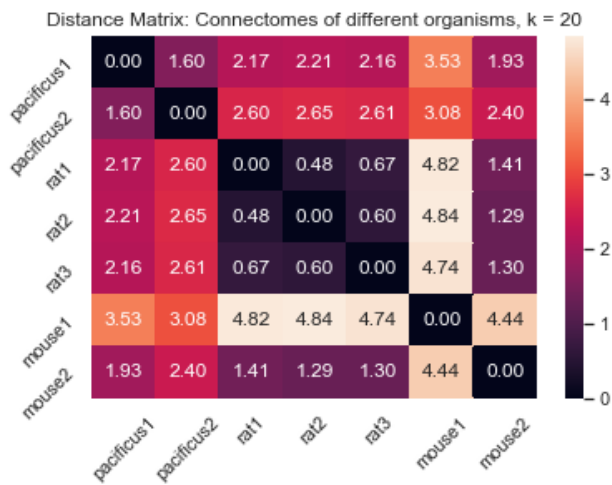


Figure 7. Heatmap of ELD distance matrix between connectomes

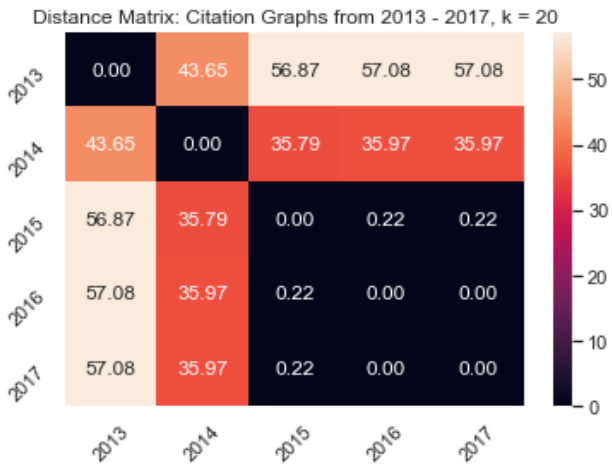


Figure 8. Heatmap of ELD distance matrix of collaboration network over 2013-2017

ELD approach on the underlying undirected graph of the digraph, but this discards orientation information. Another approach is to take the directed version of the Laplacian (Chung, 2005) and develop analogous embeddings.

Labelled Graphs ELD could also be extended to comparing vertex-labelled graphs, where there are known correspondences between vertices. The most natural way to do this is to retain the vertex correspondences after performing the Laplacian embedding, and compute a distance in Euclidean space between the matching vertices.

Computational efficiency is one of the advantages of adopting the ERD approach. The most computationally intensive step in ELD is eigendecomposition, which we have implemented using standard numerical libraries and methods. It is possible to achieve substantial speedups in practice by using sparse numerical techniques or a myriad of other approximation/optimization schemes. For applications with repeated calculations on the same graphs (e.g. calculating a distance matrix), the embedded representation can be stored and retrieved for more efficient computation. A version of the ELD based on sparse numerical computations is provided in the supplementary code. The sparse version provides substantial speedups when the graphs involved are large (e.g. > 10000 vertices).

One major design choice made in the definition of the ELD is by using the combinatorial Laplacian rather than the normalized Laplacian $\mathbf{I} - \mathbf{D}^{-1/2} \mathbf{A} \mathbf{D}^{-1/2}$. The ELD definition and implementation described above could easily be extended to the normalized Laplacian case, and virtually all of our theoretical results will carry over. While the combinatorial Laplacian approach naturally takes scale information of the graphs into account, the normalized Laplacian does not. Depending on the context of the application, users might find either forms of the Laplacian to be more appropriate.

In figure 6, we observed that the NPD distance matrix did not show block structure, but instead shows an interesting checkerboard structure for comparing rings-of-cliques. One hypothesis that this suggests is the NPD might be capturing the size of the cliques locally, rather than the number of cliques/communities globally.

The focus of this paper is mainly to introduce the ELD as a novel distance between graphs of different scales. There are many downstream machine learning/statistics tasks that one could potentially perform with the ELD, and we delegate these investigations to future research.

References

Bagrow, J. P. and Boltt, E. M. An information-theoretic, all-scales approach to comparing networks. *Applied Network Science*, 4(1):1–15, 2019.

- Belkin, M. and Niyogi, P. Laplacian eigenmaps for dimensionality reduction and data representation. *Neural computation*, 15(6):1373–1396, 2003.
- Berlingerio, M., Koutra, D., Eliassi-Rad, T., and Faloutsos, C. Netsimile: A scalable approach to size-independent network similarity. *arXiv preprint arXiv:1209.2684*, 2012.
- Bock, D. D., Lee, W.-C. A., Kerlin, A. M., Andermann, M. L., Hood, G., Wetzel, A. W., Yurgenson, S., Soucy, E. R., Kim, H. S., and Reid, R. C. Network anatomy and in vivo physiology of visual cortical neurons. *Nature*, 471(7337):177–182, 2011.
- Bonneel, N., Rabin, J., Peyré, G., and Pfister, H. Sliced and radon wasserstein barycenters of measures. *Journal of Mathematical Imaging and Vision*, 51(1):22–45, 2015.
- Bonnotte, N. *Unidimensional and evolution methods for optimal transportation*. PhD thesis, Paris 11, 2013.
- Borgwardt, K., Ghisu, E., Llinares-López, F., O’Bray, L., and Rieck, B. Graph kernels: State-of-the-art and future challenges. *arXiv preprint arXiv:2011.03854*, 2020.
- Bota, M., Dong, H.-W., and Swanson, L. W. Combining collation and annotation efforts toward completion of the rat and mouse connectomes in bams. *Frontiers in neuroinformatics*, 6:2, 2012.
- Bumbarger, D., Riebesell, M., Sommer, R., et al. System-wide rewiring underlies behavioral differences in predatory and bacterial-feeding nematodes. *Cell*, 152(1-2):109–119, 2013.
- Bunke, H. On a relation between graph edit distance and maximum common subgraph. *Pattern Recognition Letters*, 18(8):689–694, 1997.
- Chazal, F., Cohen-Steiner, D., Guibas, L. J., Méholi, F., and Oudot, S. Y. Gromov-hausdorff stable signatures for shapes using persistence. In *Computer Graphics Forum*, volume 28, pp. 1393–1403. Wiley Online Library, 2009.
- Chung, F. Laplacians and the cheeger inequality for directed graphs. *Annals of Combinatorics*, 9(1):1–19, 2005.
- Dehmer, M. M., Barbarini, N. N., Varmuza, K. K., and Graber, A. A. Novel topological descriptors for analyzing biological networks. *BMC structural biology*, 10(1):1–17, 2010.
- Donnat, C. and Holmes, S. Tracking network dynamics: A survey of distances and similarity metrics. *arXiv preprint arXiv:1801.07351*, 2018.
- Durante, D., Dunson, D. B., and Vogelstein, J. T. Non-parametric bayes modeling of populations of networks. *Journal of the American Statistical Association*, 112(520):1516–1530, 2017.
- Edwards, D. A. The structure of superspace. In *Studies in topology*, pp. 121–133. Elsevier, 1975.
- Emmert-Streib, F., Dehmer, M., and Shi, Y. Fifty years of graph matching, network alignment and network comparison. *Information sciences*, 346:180–197, 2016.
- Gao, X., Xiao, B., Tao, D., and Li, X. A survey of graph edit distance. *Pattern Analysis and applications*, 13(1):113–129, 2010.
- Gärtner, T., Flach, P., and Wrobel, S. On graph kernels: Hardness results and efficient alternatives. In *Learning theory and kernel machines*, pp. 129–143. Springer, 2003.
- Ghosh, S., Das, N., Gonçalves, T., Quaresma, P., and Kundu, M. The journey of graph kernels through two decades. *Computer Science Review*, 27:88–111, 2018.
- Ginestet, C. E., Li, J., Balachandran, P., Rosenberg, S., Kolaczyk, E. D., et al. Hypothesis testing for network data in functional neuroimaging. *Annals of Applied Statistics*, 11(2):725–750, 2017.
- Grindrod, P. and Lee, T. Comparison of social structures within cities of very different sizes. *Royal Society open science*, 3(2):150526, 2016.
- Gromov, M. Groups of polynomial growth and expanding maps. *Publications Mathématiques de l’Institut des Hautes Études Scientifiques*, 53(1):53–78, 1981.
- Gromov, M. *Metric structures for Riemannian and non-Riemannian spaces*. Springer Science & Business Media, 2007.
- Hagberg, A., Swart, P., and S Chult, D. Exploring network structure, dynamics, and function using networkx. Technical report, Los Alamos National Lab.(LANL), Los Alamos, NM (United States), 2008.
- Jeong, H., Qian, X., and Yoon, B.-J. Effective comparative analysis of protein-protein interaction networks by measuring the steady-state network flow using a markov model. In *BMC bioinformatics*, volume 17, pp. 15–27. BioMed Central, 2016.
- Kaiser, M. A tutorial in connectome analysis: topological and spatial features of brain networks. *Neuroimage*, 57(3):892–907, 2011.
- Ketkar, N. S., Holder, L. B., and Cook, D. J. Faster computation of the direct product kernel for graph classification. In *2009 IEEE Symposium on Computational Intelligence and Data Mining*, pp. 267–274. IEEE, 2009.

- Kolouri, S., Nadjahi, K., Simsekli, U., Badeau, R., and Rohde, G. K. Generalized sliced wasserstein distances. *arXiv preprint arXiv:1902.00434*, 2019.
- Kolouri, S., Naderializadeh, N., Rohde, G. K., and Hoffmann, H. Wasserstein embedding for graph learning. *arXiv preprint arXiv:2006.09430*, 2020.
- Koutra, D., Vogelstein, J. T., and Faloutsos, C. Deltacon: A principled massive-graph similarity function. In *Proceedings of the 2013 SIAM International Conference on Data Mining*, pp. 162–170. SIAM, 2013.
- Kriege, N. M., Johansson, F. D., and Morris, C. A survey on graph kernels. *Applied Network Science*, 5(1):1–42, 2020.
- Lee, J. R., Gharan, S. O., and Trevisan, L. Multiway spectral partitioning and higher-order cheeger inequalities. *Journal of the ACM (JACM)*, 61(6):1–30, 2014.
- Louis, A., Raghavendra, P., Tetali, P., and Vempala, S. Many sparse cuts via higher eigenvalues. In *Proceedings of the forty-fourth annual ACM symposium on Theory of computing*, pp. 1131–1140, 2012.
- Lunagómez, S., Olhede, S. C., and Wolfe, P. J. Modeling network populations via graph distances. *Journal of the American Statistical Association*, pp. 1–18, 2020.
- Maretic, H. P., Gheche, M. E., Chierchia, G., and Frossard, P. Got: An optimal transport framework for graph comparison. *arXiv preprint arXiv:1906.02085*, 2019.
- Mémoli, F. On the use of gromov-hausdorff distances for shape comparison. 2007.
- Nadjahi, K., Durmus, A., Jacob, P. E., Badeau, R., and Simsekli, U. Fast approximation of the sliced-wasserstein distance using concentration of random projections. *Advances in Neural Information Processing Systems*, 34, 2021.
- Ng, A., Jordan, M., and Weiss, Y. On spectral clustering: Analysis and an algorithm. *Advances in neural information processing systems*, 14:849–856, 2001.
- Nikolentzos, G., Siglidis, G., and Vazirgiannis, M. Graph kernels: A survey. *arXiv preprint arXiv:1904.12218*, 2019.
- Oles, V., Lemons, N., and Panchenko, A. Efficient estimation of a gromov–hausdorff distance between unweighted graphs. *arXiv preprint arXiv:1909.09772*, 2019.
- Rabin, J., Peyré, G., Delon, J., and Bernot, M. Wasserstein barycenter and its application to texture mixing. In *International Conference on Scale Space and Variational Methods in Computer Vision*, pp. 435–446. Springer, 2011.
- Richiardi, J., Achard, S., Bunke, H., and Van De Ville, D. Machine learning with brain graphs: predictive modeling approaches for functional imaging in systems neuroscience. *IEEE Signal Processing Magazine*, 30(3):58–70, 2013.
- Saad-Eldin, A., Pedigo, B. D., Priebe, C. E., and Vogelstein, J. T. Graph matching via optimal transport. *arXiv preprint arXiv:2111.05366*, 2021.
- Sanfeliu, A. and Fu, K.-S. A distance measure between attributed relational graphs for pattern recognition. *IEEE transactions on systems, man, and cybernetics*, (3):353–362, 1983.
- Sharpnack, J., Singh, A., and Rinaldo, A. Changepoint detection over graphs with the spectral scan statistic. In *Artificial Intelligence and Statistics*, pp. 545–553. PMLR, 2013.
- Shi, J. and Malik, J. Normalized cuts and image segmentation. *IEEE Transactions on pattern analysis and machine intelligence*, 22(8):888–905, 2000.
- Soundarajan, S., Eliassi-Rad, T., and Gallagher, B. A guide to selecting a network similarity method. In *Proceedings of the 2014 Siam international conference on data mining*, pp. 1037–1045. SIAM, 2014.
- Spielman, D. Spectral and algebraic graph theory. 2019.
- Tantardini, M., Ieva, F., Tajoli, L., and Piccardi, C. Comparing methods for comparing networks. *Scientific reports*, 9(1):1–19, 2019.
- Vayer, T., Chapel, L., Flamary, R., Tavenard, R., and Courty, N. Optimal transport for structured data with application on graphs. *arXiv preprint arXiv:1805.09114*, 2018.
- Villani, C. *Optimal transport: old and new*, volume 338. Springer, 2009.
- Vishwanathan, S. V. N., Schraudolph, N. N., Kondor, R., and Borgwardt, K. M. Graph kernels. *Journal of Machine Learning Research*, 11:1201–1242, 2010.
- Vogelstein, J. T., Perlman, E., Falk, B., Baden, A., Roncal, W. G., Chandrashekar, V., Collman, F., Seshamani, S., Patsolic, J. L., Lillaney, K., et al. A community-developed open-source computational ecosystem for big neuro data. *Nature methods*, 15(11):846–847, 2018.
- Von Luxburg, U. A tutorial on spectral clustering. *Statistics and computing*, 17(4):395–416, 2007.
- Wills, P. and Meyer, F. G. Metrics for graph comparison: a practitioner’s guide. *PloS one*, 15(2):e0228728, 2020.

Wilson, R. C. and Zhu, P. A study of graph spectra for comparing graphs and trees. *Pattern Recognition*, 41(9): 2833–2841, 2008.

Xu, H., Luo, D., Zha, H., and Carin, L. Gromov-wasserstein learning for graph matching and node embedding. In *International conference on machine learning*, pp. 6932–6941. PMLR, 2019.

Zeng, Z., Tung, A. K., Wang, J., Feng, J., and Zhou, L. Comparing stars: On approximating graph edit distance. *Proceedings of the VLDB Endowment*, 2(1):25–36, 2009.

A. Appendix

A.1. Proof of pseudometric property of ELD

Proof. To show that the ELD $\rho_k(\cdot, \cdot)$ is a pseudometric, we have to check four properties. Our arguments hold for all admissible k as specified in the definition of the ELD in section 3.

1. **Nonnegativity:** $\rho_k(\cdot, \cdot) \geq 0$. Note that $\mathcal{W}_p(\cdot, \cdot) \geq 0$ since it is a metric. Since $\rho_k(G, H)$ is simply a finite, non-negatively weighted average of $\mathcal{W}_p(\cdot, \cdot)$ terms, ρ_k will also be non-negative.
2. **Symmetry:** $\rho_k(G, H) = \rho_k(H, G)$ for any graphs G, H . Note that since $\mathcal{W}_p(\cdot, \cdot)$ is a metric, it is also symmetric. Since $\rho_k(G, H)$ is just a finite, non-negatively weighted average of symmetric $\mathcal{W}_p(\cdot, \cdot)$ terms, with the first argument of \mathcal{W}_p dependent only on G and the second argument of \mathcal{W}_p dependent only on H , conclude that $\rho_k(G, H)$ is also symmetric.
3. **Identity of indiscernibles:** $\rho_k(G, G) = 0$. (since this is a pseudometric, we allow for the possibility that there exist $G \neq H$ where $\rho_k(G, H) = 0$). To show this, simply note that \mathcal{W}_p is a metric, hence $\mathcal{W}_p(a, a) = 0$ for any $a = a$. Since $\rho_k(G, G)$ is just the finite, non-negatively weighted average of $\mathcal{W}_p(\cdot, \cdot)$ terms where the two arguments in each \mathcal{W}_p term will be identical, conclude that each of the \mathcal{W}_p terms will be 0 and hence $\rho_k(G, G) = 0$.
4. **Triangle inequality:** $\rho_k(G_1, G_2) + \rho_k(G_2, G_3) \geq \rho_k(G_1, G_3)$ for graphs G_1, G_2, G_3 . To show the triangle inequality, again leverage the fact that \mathcal{W}_p is a metric to obtain the inequality $\mathcal{W}_p(a, b) + \mathcal{W}_p(b, c) \geq \mathcal{W}_p(a, c)$ for any a, b, c .

Get:

$$\begin{aligned}
 & \rho(G_1, G_2) + \rho(G_2, G_3) \\
 &= \frac{1}{k} \sum_{r=1}^k \mathcal{W}_p(\lambda_r^{G_1} \text{proj}_{\mathbf{e}_r}(\mu_{\mathcal{X}_{G_1}}), \lambda_r^{G_2} \text{proj}_{\mathbf{e}_r}(\mu_{\mathcal{X}_{G_2}})) + \frac{1}{k} \sum_{r=1}^k \mathcal{W}_p(\lambda_r^{G_2} \text{proj}_{\mathbf{e}_r}(\mu_{\mathcal{X}_{G_2}}), \lambda_r^{G_3} \text{proj}_{\mathbf{e}_r}(\mu_{\mathcal{X}_{G_3}})) \\
 &= \frac{1}{k} \sum_{r=1}^k (\mathcal{W}_p(\lambda_r^{G_1} \text{proj}_{\mathbf{e}_r}(\mu_{\mathcal{X}_{G_1}}), \lambda_r^{G_2} \text{proj}_{\mathbf{e}_r}(\mu_{\mathcal{X}_{G_2}})) + \mathcal{W}_p(\lambda_r^{G_2} \text{proj}_{\mathbf{e}_r}(\mu_{\mathcal{X}_{G_2}}), \lambda_r^{G_3} \text{proj}_{\mathbf{e}_r}(\mu_{\mathcal{X}_{G_3}}))) \\
 &\geq \frac{1}{k} \sum_{r=1}^k \mathcal{W}_p(\lambda_r^{G_1} \text{proj}_{\mathbf{e}_r}(\mu_{\mathcal{X}_{G_1}}), \lambda_r^{G_3} \text{proj}_{\mathbf{e}_r}(\mu_{\mathcal{X}_{G_3}})) = \rho(G_1, G_3)
 \end{aligned}$$

□

A.2. Proof of invariance under graph isomorphism

Proof. Given a graph G , a permutation σ on its vertices $[n]$, and the corresponding permutation matrix \mathbf{P}_σ , it is well known fact (Spielman, 2019) that

$$L_{G_\sigma} = \mathbf{P}_\sigma \mathbf{L}_G \mathbf{P}_\sigma^T$$

It then follows directly by associativity that:

$$\mathbf{L}_{G_\sigma} \mathbf{v} = \lambda \mathbf{v} \Leftrightarrow (\mathbf{P}_\sigma \mathbf{L}_G \mathbf{P}_\sigma^T)(\mathbf{P}_\sigma \mathbf{v}) = \lambda (\mathbf{P}_\sigma \mathbf{v}) \quad (1)$$

This shows that the Laplacian eigenvectors of the permuted graph is simply the eigenvectors of the original graph permuted the same way. This also shows that eigenvalues are unchanged by graph isomorphisms/permutations.

The ELD by definition computes a distance between the (eigenvalue-weighted) empirical measures associated with the Laplacian embeddings of two respective graphs. Since eigenvalues are invariant under graph isomorphism, it suffices for us to show that the (unweighted) empirical measure associated with the Laplacian embedding of a graph is invariant under graph isomorphisms/permutations.

Consider the (unweighted) empirical measure for G projected along the canonical Euclidean axis \mathbf{e}_r :

$$\text{proj}_{\mathbf{e}_r} \mu_{\mathcal{X}_G} = \frac{1}{n} \sum_{i=1}^n \delta_{\mathbf{x}_i^G(r)}$$

and the (unweighted) empirical measure for G_σ projected along the canonical Euclidean axis \mathbf{e}_r :

$$\begin{aligned}\text{proj}_{\mathbf{e}_r} \mu_{\mathcal{Y}_{G_\sigma}} &= \frac{1}{n} \sum_{i=1}^n \delta_{\mathbf{y}_i^{G_\sigma}(r)} = \frac{1}{n} \sum_{i=1}^n \delta_{\mathbf{v}_r^{G_\sigma}(i)} \\ &= \frac{1}{n} \sum_{i=1}^n \delta_{\mathbf{P}_\sigma \mathbf{v}_r^G(i)} = \frac{1}{n} \sum_{i=1}^n \delta_{(\mathbf{P}_\sigma \mathbf{x}^G)_i(r)}\end{aligned}$$

The effect of the permutation is just changing the order of addition of the entries in \mathbf{x} under a fixed r , and since we are only considering finite sums, the order of addition does not affect the sum.

This shows that the (unweighted) empirical measure associated with the Laplacian embedding of a graph is invariant under graph isomorphisms, which proves the desired claim. \square